Imaging H abstraction dynamics in crossed molecular beams: O(^{3}P) + propanol isomers

Journal:	*Physical Chemistry Chemical Physics*
Manuscript ID	CP-ART-10-2018-006351.R1
Article Type:	Paper
Date Submitted by the Author:	11-Nov-2018
Complete List of Authors:	Li, Hongwei; University of Missouri Columbia College of Arts and Science, Chemistry Kamasah, Alexander; University of Missouri Columbia College of Arts and Science, Chemistry Suits, Arthur; University of Missouri Columbia College of Arts and Science, Chemistry

Imaging H abstraction dynamics in crossed molecular beams: $O(^3P)$ + propanol isomers

Hongwei Li, Alexander Kamasah, Arthur G. Suits*
Department of Chemistry, University of Missouri Columbia, MO 65211, United States

ABSTRACT

The crossed beam reaction dynamics of ground state $O(^3P)$ atoms with propanol isomers (1-propanol and 2-propanol) have been studied for the first time using the velocity map imaging technique. The hydroxypropyl radical products, generated from H-abstraction of the secondary and tertiary C-H groups of propanol isomers, were detected via single photon ionization at 157 nm under single collision conditions with collision energies of 8 and 10 kcal mol^{-1}. Direct rebound dynamics were suggested by the angular distributions, which show overall sideways-backward scattering but more pronounced backward scattering for both isomer reactions under all collision energies studied here. All the translational energy distributions peak at low energy, on average 20%-40% of the total available energy. This indicates high internal excitation in the products that is treated by various models of energy release. We infer that most of the total available energy is partitioned into rotational excitation due to the long-rang dipole-dipole interaction between the dipolar OH and hydroxypropyl radicals.

*Author to whom correspondence should be addressed: suitsa@missouri.edu

INTRODUCTION

There has been keen interest in prototypical polyatomic reactions of atomic oxygen with hydrocarbons and they have been extensively studied both experimentally and theoretically for decades. A good understanding of this family of elementary reactions is important for successful development of accurate modeling for combustion, atmospheric, and interstellar chemistry.[1-3] It is well known that reactions involving the electronically excited oxygen O(^{1}D) have large cross sections and usually undergo insertion with no barrier. In contrast, ground state oxygen O(^{3}P) reactions have smaller cross sections and may participate in direct abstraction or addition-elimination pathways depending on the nature of the co-reactant.[4] Crossed molecular beam experiments allow the measurement of angular and translational energy distributions during such bimolecular reactions, providing coupling information between scattering angles and energy partitioning into translational and internal degrees of freedom of the products.[5] Combined with theoretical calculations these provide direct insight into the underlying mechanisms of elementary chemical reactions of interest.[5-7]

Direct abstraction by ground state atomic O(^{3}P) reaction normally occurs with compounds that contain less strongly bound hydrogen atoms such as aldehydes, or with saturated compounds such as alkanes, alcohols, etc.[8] One of the major products for the direct H abstraction mechanism is hydroxyl radical, OH ($^2\Pi$), which enables experimental dynamics study on these reactions via the well-known laser induced fluorescence (LIF) detection of OH radical. The first comprehensive H abstraction dynamics study of O(^{3}P) reaction with saturated hydrocarbons was done by Andresen and Luntz in 1980.[9, 10] They applied an effusive O atom source into a crossed beam apparatus and measured the nascent internal state distributions of OH products via LIF probe. A variety of target hydrocarbon reagents was used to investigate the different dynamics of abstraction reaction with primary, secondary or tertiary hydrogen atoms. They detected rotationally cold OH products regardless of type of H abstracted: all the rotational distributions peaked at the lowest rotational quantum number and dropped quickly thereafter. However, the observed vibrational state distribution of OH depended significantly on the type of H abstraction site, with vibrational excitation increasing dramatically in going from primary, secondary, to tertiary H atom target. They demonstrated a collinear O-H-C abstraction mechanism that was also supported by quasi-classical trajectory calculations on a model triatomic London-Eyring-Polanyi-Sato potential surface to simulate reaction with a secondary H atom. This triatomic picture has been able to account quite well for the observations in the later work by Whitehead group[11] and McKendrick group[8, 12] again using LIF probe of the OH products.

In 2000, Kajimoto and co-workers studied the dynamics of O(^{3}P) reaction with cyclohexane and isobutane by measuring differential cross sections (DCSs) of the OH $v = 1$ product using Doppler-resolved polarization spectroscopy in a "PHOTOLOC" type of experiment.[13] At low collision energy, they observed a backscattered angular distribution as was predicted in the original theoretical studies by Luntz and Andresen. However, when collision energy increased, the forward scattering component became comparable to the backward scattering, which indicates the large impact parameter collisions (i.e. stripping pathway) contribute here to the reactive scattering. Moreover, significant internal excitation in the alkyl radical products was inferred, meaning that the alkyl radical does not behave as a spectator as assumed in the collinear triatomic picture. Two years later, Suits and coworkers carried out a crossed beam study on the reactions of O(^{3}P) with alkanes (cyclohexane, n-butane and isobutane) at a range of well-defined collision energies from 4.7 to 14.8 kcal mol^{-1} using velocity map imaging of the alkyl radical product via single photon ionization at 157 nm.[14] Largely

backscattered alkyl radical products were observed at all collision energies and the scattering distribution was broadened with increasing collision energy, consistent with the picture of direct rebound dynamics by Luntz and Andresen. More interestingly, the large fraction of the available energy was inferred to be partitioned into internal degrees of freedom of the alkyl radical that cannot be fully explained by the simple triatomic picture of the reaction. They proposed a modification of the triatomic model in which the exoergicity is adjusted to reflect "vertical" rather than "adiabatic" H abstraction energetics. Briefly, the old bond breaking and new bond forming during the abstraction process are too rapid so that the alkyl radical does not have enough time to relax to its minimum energy geometry, resulting in certain amount of energy "locked" into the alkyl radical moiety.

The energy partitioning among the products during the bimolecular reaction is also impacted by the post-transition state dynamics where there are dipole-dipole interactions if two products are polar species. Orr-Ewing and coworkers found this effect in the H abstraction reactions of Cl atoms with functionalized organic molecules, such as alcohols, ethers, and amines.[15-18] So far without exception, all H abstractions by Cl atoms from alkanes are observed to result in rotationally cold HCl products due to the collinear geometries for the C-H-Cl moiety in the transition states in all the systems investigated.[15] However, more rotational excitation of HCl products are found from the H abstractions of Cl with functionalized organic molecules, such as methanol, ethanol, dimethyl ether, and methylamine.[16-18] The enhanced rotation of HCl products arises from anisotropic interactions in the exit channel between the dipolar HCl and radical fragments despite of the collinear Cl-H-C transition moiety. The is also supported by on-the-fly *ab initio* dynamics calculations of reaction trajectories that closely reproduce the angular momentum quantum number of the HCl molecules at the peak of the measured rotational distribution.[16] Very recently, our group studied the bimolecular reaction dynamics of O(^{3}P) reaction with aliphatic amines and observed fast intersystem crossing occurring in the exit channel, promoted by the dipole-dipole interaction from the polar product pair and degenerate surfaces with strong spin-orbit coupling.[19]

Here, we present the latest results of our crossed-beam study on the reaction dynamics of the ground state atomic oxygen O(^{3}P) with 1-propanol and 2-propanol. The product hydroxyalkyl radicals were probed via single photon ionization at 157 nm and their images recorded and analyzed after density-flux correction and background subtraction. The coupled translational energy distributions and center-of-mass angular distributions are derived directly from the images. The underlying dynamics are understood by the help of electronic structure calculations and energy partitioning during the reaction is discussed by various models.

EXPERIMENTAL SECTION

The scattering experiments were carried out in a crossed molecular beam apparatus[20] combined with a DC slice ion imaging[21-23], which has been previously described elsewhere.[24] The apparatus consists of a reaction chamber and two source chambers that are perpendicular to each other. Both molecular beams were produced in a separate supersonic expansion in the two source chambers ($\sim 10^{-7}$ torr base pressure and $\sim 10^{-5}$ torr operational pressure) and skimmed into the reaction chamber. Photolysis of SO_2 by a 193 nm excimer laser was used to generate O (^{3}P) atom and it is known that this does not produce any O (^{1}D).[25, 26] A 5% SO_2 (≥99.9%, Sigma-Aldrich) seeded in He was pulsed from a piezoelectric stack valve [31] with a 120 μm translational actuator and 50 μs pulse duration. A 1 mm diameter capillary tube was mounted on the exit of the nozzle plate of the stack valve, and 193 nm radiation (15 mJ/pulse from a GAM

ArF excimer laser) was loosely focused onto the capillary to photolyze SO_2 to generate a very intense O(^{3}P) beam. Another piezoelectric disc valve was used to pulse the 1-propanol or 2-propanol (≥99.9%, Sigma-Aldrich) molecular target beam. By seeding them 5% in He or H_2, the collision energy was changed from 8 kcal mol^{-1} to 10 kcal mol^{-1}. The scattered hydroxyalkyl radical products were ionized with a F_2 excimer laser (157 nm, 7.9 eV, ~1 mJ/pulse). The resultant ions were then accelerated via a four-electrode dc slice ion optics assembly to impact on a dual microchannel plate (MCP) detector coupled to a fast phosphor screen. The detector was gated for the center slice of the scattered product ions and the resultant images were recorded using a charge-coupled device (CCD) camera and analyzed with our data acquisition program[27-29]. Background subtraction and density-to-flux corrections were performed prior to transforming the scattering distributions into the center-of mass coordinate. Background images were recorded sequentially rather than shot-to-shot, but the conditions were stable so reliable subtraction conditions could be obtained.

CALCULATION METHODS

Ab initio calculations (including geometric structure and energy, and ionization energy calculation) were performed using the CBS-QB3 and wB97XD/6-311+G(2d,p) level of theory with geometries optimized at the same level, implemented in the Gaussian16 quantum chemistry software package[30]. Connections between the TS and local minima were verified by intrinsic reaction coordinate (IRC) calculations at the B3LYP/6-311G(2d,d,p) and wB97XD/6-311+G(2d,p) level of theory. The energies of the transition states for both O(^{3}P) reactions with 1-propanol and 2-propanol were also calculated by CCSD(T)/cc-pVTZ level of theory using the B2PLYPD3/cc-pVTZ optimized geometries and vibrational frequencies for comparison.

RESULTS

The crossed-molecular beam technique coupled with single photon ionization and DC slice ion imaging detection has been shown to be a sensitive technique to investigate bimolecular reactions dynamics.[24, 31-36] In probing the hydroxyalkyl radical using our 157 nm excimer laser, we need to take into account the detection efficiency for various radical products from the particular hydrogen abstraction sites.[37] Both propanol isomers have two distinct abstraction sites: one at the hydroxyl end of the molecule and the other involving primary, secondary, and tertiary C-H groups. Figure 1 presents the reaction enthalpies (at 0 K, blue numbers in unit of kcal mol^{-1}) for H abstraction by O(^{3}P) at the indicated sites, and the vertical ionization energies (black numbers in parentheses, in unit of eV) of the corresponding product radicals. The stationary point geometries for propanol isomers and their H abstraction radical products are optimized and their energies are calculated at the CBS-QB3 level of theory. Even though H abstractions from both hydroxyl group and C-H groups are energetically accessible according to the reaction enthalpies, the vertical ionization energy calculations indicate selectivity on the radical products that we can detect with our

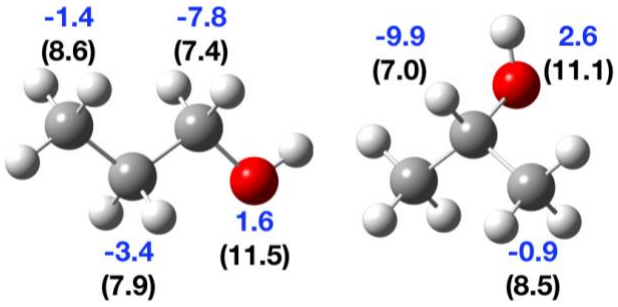

Figure 1. Lowest energy structures of 1-propanol (left) and 2-propanol (right). Reaction enthalpies at 0 K (numbers in blue color, kcal mol^{-1}) at different abstraction sites are calculated at CBS-QB3 level of theory. Numbers in parenthesis are vertical ionization energies (eV) of corresponding product radicals.

single photon ionization (7.9 eV). For 1-propanol, the ionization energy of the H abstraction product from the OH group and primary C-H group is higher than our detection probe of 7.9 eV, while the abstraction product from the secondary C-H group is lower. Thus, the radical products of the H abstraction on the α- and β-H sites are detected in the present work for 1-propanol. Analogously, for 2-propanol, we only detect the β-H abstraction radical product that is on the tertiary C-H group.

O(^{3}P) + 1-propanol

The reactive scattering images of the 1-hydroxypropyl radical products from the reaction of O(^{3}P) with 1-Propanol at collision energies (E_c) of 8.1 and 10.2 kcal mol^{-1} (with the Newton diagrams superimposed on them) are shown in the left panels of Figure 2. The 1-hydroxypropyl radical that we are probing here is produced from H-abstraction from the α- and β-H sites of 1-propanol as we mentioned earlier. We performed background subtraction by recording images with the 193 nm photolysis laser off and the 157 nm probe laser on to isolate the reactive scattering signals from the radicals produced by the photodissociation of 1-propanol at 157 nm. Unfortunately, the intense photochemical signal creates substantial noise and brings uncertainty in the reactive flux of the forward component. For this reason, we omitted the first 45° of the forward component in the further analysis for this O(^{3}P) + 1-propanol reaction. The right panels of Figure 2 show the corresponding global translational kinetic energy and center-of-mass angular distributions at two different collision energies (E_c = 8.1 kcal mol^{-1} in black and E_c = 10.2 kcal mol^{-1} in red). The average translational energy released at the collision energy of 10.2 kcal mol^{-1} and 8.1 kcal mol^{-1} is 5.3 and 3.5 kcal mol^{-1}, respectively. The angular distributions at both collision energies show both sideways and backward scattering with respect to the direction of the propanol beam but backward scattering is dominant.

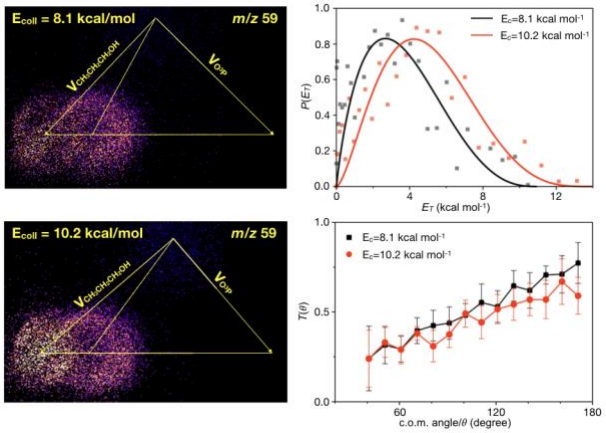

Figure 2. Sliced scattering images for the reaction of O(^{3}P) with 1-propanol (Newton diagrams superimposed on them) under collision energy of 8.1(left top panel) and 10.2 (left bottom panel) kcal mol^{-1}, and their corresponding global translational energy release (P(E_T), right top panel) and center-of-mass angular (T(θ), right bottom panel) distributions. The T(θ) distributions are shown averaged every 10° with error bars (±σ) estimated by mean absolute deviation of the raw data in the corresponding angle range.

O(^{3}P) + 2-propanol

The left panels of Figure 3 show the sliced reactive scattering images of 2-hydroxy-2-propyl radical products for the O(^{3}P) + 2-propanol reaction at collision energies of 8.3 kcal mol^{-1} (top) and 10.0 kcal mol^{-1} (bottom). For this reaction, the 2-hydroxy-2-propyl radical products that we probed here are only produced from H-abstraction from α-H sites of 2-propanol according to the ionization energy calculations. The total available energy for this reaction is 18.2 and 19.9 kcal mol^{-1} for collision energies of 8.3 and 10.0 kcal mol^{-1}, respectively. Just as for the 1-propanol reaction, due to the large background interference in the forward direction, we have omitted the first 45° component in the further analysis for this O(^{3}P) + 2-propanol reaction

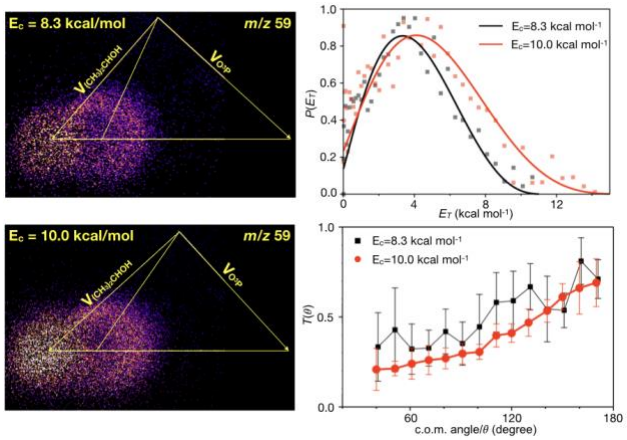

Figure 3. Sliced scattering images for the reaction of O(^{3}P) with 2-propanol under collision energy of 8.3(left top panel) and 10.0 (left bottom panel) kcal mol^{-1}, and their corresponding global translational energy release ($P(E_T)$, right top panel) and center-of-mass angular ($T(\theta)$, right bottom panel) distributions. The $T(\theta)$ distributions are shown averaged very 10° with error bars ($\pm\sigma$) estimated by mean absolute deviation of the raw data in the corresponding angle range.

as well. The global translational energy release distributions are given in the right top panel of Figure 3, showing average translational energy of 4.2 and 5.4 kcal mol^{-1} for the collision energy of 8.3 and 10.0 kcal mol^{-1} accounting for 23% and 27% of the total available energy, respectively. The center-of-mass angular distributions of both collision energies are shown in the right bottom panel of Figure 3, indicating again more pronounced backward scattering with respect to the propanol beam direction.

Potential energy profiles

The key stationary points on the triplet potential energy surfaces of the O (^{3}P) reactions with 1-propanol and 2-propanol were optimized and their energies calculated via CBS-QB3 and wB97XD/6-311+G(2d,p) levels of theory. Both methods give similar results as shown in Figure 4. For the O(^{3}P) + 1-propanol reaction, two H abstraction product channels are detectable with our 157 nm photoionization probe from the two secondary C-H sites. The transition states (TSs) of both product channels are found to have collinear O-H-C structure (∠OHC=173.2° for α-H TS and ∠OHC=172.1° for β-H TS) at the CBS-QB3 level of theory. The H abstraction from the α-H site has lower barrier than the β-H site calculated by both CBS-QB3 and wB97XD/6-311+G(2d,p) methods as shown in Figure 4. However, considering the uncertainty from both calculation methods, the absolute barrier heights are hard to calculate accurately since the they are so close to the reactant asymptotic limit in energy. T_1-diagnostic values at CCSD(T)/cc-pVTZ level were examined to check the multireference character of both H abstraction TSs and have found T_1-diagnostics in the range of 0.015-0.018. T_1-diagnostics larger than 0.02 suggests the multireference nature of the wave functions.[38] We then calculated the TS energy of both H abstraction channels by the CCSD(T)/cc-pVTZ method at the B2PLYPD3/cc-pVTZ optimized geometries. The TS of the α-H abstraction has lower barrier of 4.2 kcal mol^{-1}, whereas TS of the β-H abstraction has higher barrier of 7.3 kcal mol^{-1} that is just below our collision energy. Therefore, the α-H abstraction is the major product channel as it is confirmed by checking with the partially deuterated 1-propanol, $CH_3CH_2CD_2OH$. For the O(^{3}P) + 2-propanol reaction, a similar collinear O-H-C (171.0° at CBS-QB3 level) transition state was located with almost no energy barrier from the 3 different methods applied here. Both propanol isomer reactions have post-TS complexes that are bound by 3-5 kcal mol^{-1}. This is due to the dipole-dipole interaction between the dipolar OH and hydroxypropyl product radicals as will be discussed later.

DISCUSSION

The reaction of ground state atomic oxygen with 1-propanol and 2-propanol has been studied with kinetic methods and the reaction rates of the H-abstraction from C-H group were

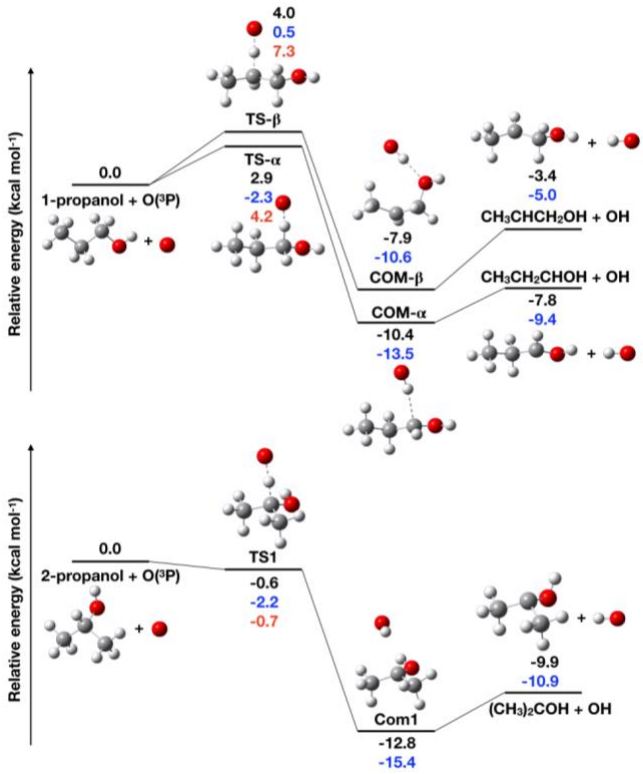

Figure 4. Key stationary points on the triplet potential energy surfaces of the O(^{3}P) + 1-propanol (top) and O(^{3}P) + 2-propanol (bottom) reactions. All energies are relative to the reactant asymptotic limits with zero point correction for various model chemistries. CBS-QB3 results are in black, wB97XD/6-311+G(2d,p) in blue, CCSD(T)/cc-pVTZ using the B2PLYPD3/cc-pVTZ geometries in red. Structures shown are from CBS-QB3 calculations.

measured.[39] The activation energy of both reactions was measure to be 12.5 and 9.1 kJ mol^{-1} for 1-propanol and 2-propanol, respectively. 2-propanol has lower activation energy due to the weaker bond of its tertiary C-H group. Nearly constant pre-exponential factors were measured for the reactions of atomic oxygen with methanol, ethanol and propanol isomers, suggesting that there is no significant steric effect on the rate constant for the title reactions of O(^{3}P) with propanol isomers. The present work represents the further details of the underlying dynamics of the hydrogen abstraction for the oxygen atom O(^{3}P) + propanol isomer reactions. The global differential cross sections as well as the translational energy partitioning were measured for the first time of these two reactions.

The angular distributions for both reactions under collision energies of 8 and 10 kcal mol^{-1} show scattering that clearly implies direct rebound dynamics. Although we are not sensitive to sharply forward-scattered products in the present work, we can rule out the forward-backward/isotropic symmetry that indicates the formation of complex during the reaction. This rebound dynamics involves small (but non-vanishing) impact parameter collisions, leading to direct reaction via a collinear transition state geometry, O-H-C, as suggested by the well-established line-of-centers triatomic model. The collinear transition state geometry, O-H-C, is also identified in both propanol isomer reactions in the stationary point calculations as discussed early in the Results section.

The product translational energy release is also measured giving important information about the dynamics. For both reactions, we replot the translational energy release distributions of the sideways (60°-120°) and backward (120°-180°) components against the collision energy as the reduced translational energy distributions (shown in Figure 5). The kinematics of a heavy-light-heavy collision show a propensity for conservation of initial collision energy into final translation, so these plots reveal the deviation from this limit. For the collision energy of both 8 and 10 kcal mol^{-1}, the similar reduced translation energy distributions are presented in the SW and BW direction, indicating that the relative energy partitioning is not sensitive to the collision energy in the energy region of the present study. The detailed average translational energy of the SW/BW components and the fraction of total energy (and collision energy) appearing in translation are summarized in Table 1. In both O(^{3}P) + propanol isomer reactions, the average translational energy release accounts for 20%-40% of the total available energy and the energy partitioning increases with increasing collision energy. A simple way to view the dynamics of

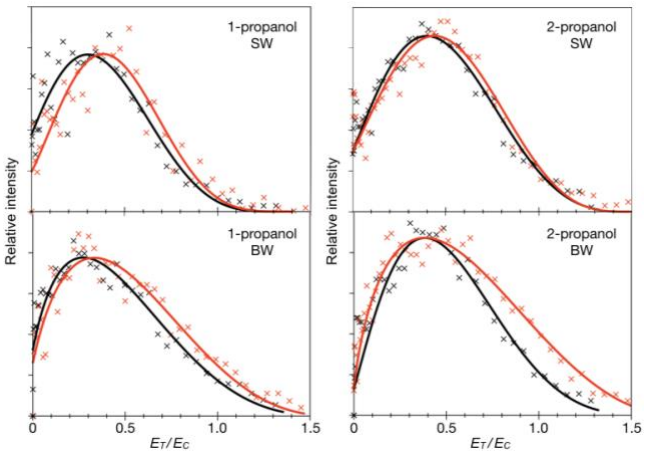

Figure 5. Reduced translational energy distributions for sideways (SW) and backward (BW) scattering components of the hydroxyalkyl products for collision energy of ~8 kcal mol^{-1} (black) and ~10 kcal mol^{-1} (red).

these reaction is an impulsive model that was widely used to understand photodissociation events. The impulsive model assumes that the total available energy is released as an impulse along the breaking bond with momentum conservation between the two "atoms" governing the translational energy release. In this model, the fraction of translational energy is simply dependent upon the mass combination: $f_T=m_{ABC}m_B/(m_{AB}m_{BC})$ for dissociation of ABC, where C is bonded to (and recoils from) B, A remains initially as a spectator.[14, 40] This model predicts an f_T of 54% of the total available energy for the O(^{3}P) + propanol systems, which is too high compared with experiment. Furthermore, this model cannot explain the collision energy dependence. The pure impulsive picture fails here since it assumes that all the energy is available for the partitioning between the fragments, which is unlikely if there is some internal excitation in recoiling fragments (*e.g.* hydroxypropyl radical product) that does not relax completely during the OH-C bond breaking.

Another simple kinematic model for the linear triatomic system suggested by Evans et al. can also be used to predict the average translational energy release: $\langle E_T \rangle = E_c\cos^2\beta + E_R\sin^2\beta$, where β is the skew angle for the reaction, E_c is the collision energy, and E_R is the reaction energy.[41] The skew angle is defined for A + BC system by $\cos^2\beta = (m_Am_B)/(m_{AB}m_{BC})$ and embodies key kinematics for the reaction. For the titled reactions, the skew angle is acute, as typically seen in heavy-light-heavy hydrogen transfer reactions, so the first term strongly dominates and predicts that the average translational energy is very close to the collision energy, which is larger than the experimental measurements. This overestimation of the translational energy from this model suggests that the internal excitation in the OH and hydroxyalkyl radical products plays an important role for the titled reactions. In this model, the remaining energy is allocated to vibrational excitation of the newly formed OH bond, therefore, it provides a rough limiting view to account for relaxation of the hydroxyalkyl radical from the TS geometry. The OH radical generated from the titled reaction could be vibrationally excited to v = 1 (OH stretch fundamental and first overtone transitions are 3570 cm^{-1} and 6974 cm^{-1}, respectively)[42] given the experimental collision energy. In the previous LIF study of the O(^{3}P) + saturated alkanes by Andresen and Luntz, the OH radical was found to be rotationally cold regardless of the nature of the alkane reagent, but vibrational excitation of OH strongly depended on the type of hydrogen abstracted. They measured the ratios of vibrational partitioning for OH ($\sigma(v = 1)/\sigma(v = 0)$) to be 0.01, 0.24 and 1.4 for primary, secondary and tertiary hydrogens, respectively.[9] Similar results were observed for the O(^{3}P) + C_2H_5OH reaction by Dutton *et al.*, where the amount of vibrational excitation of OH ($\sigma(v = 1)/\sigma(v = 0)$) is 0.22 by H abstraction from the secondary C-H bond.[43] Therefore, assuming the same branching of vibrational excitation for OH as the previous measurements, the OH vibrational excitation will account for 10%-20% of total available energy for 1-propanol reaction, and 30% for 2-propanol reaction.

Another model for estimating internal excitation of the hydroxyalkyl radicals is the "vertical" abstraction mechanism that was invoked by Liu *et al.* in O + n-butane reaction[14] and Whitney *et al.* in F + C_2H_6 reaction[44]. In this picture, the C-H bond breaks so rapidly that hydroxypropyl radical cannot relax to its minimum energy geometry, resulting in a certain amount of energy "locked" in the C_3H_6OH moiety. This view is equivalent to the Franck-Condon picture that the hydrogen transfer is a "vertical" rather than an "adiabatic" process. Some available energy will be partitioned into vibrational excitation of the hydroxypropyl radical product in a non-statistical and mode-specific manner, associated with significant structural changes between propanol parent molecule and hydroxypropyl radical product. We have optimized the TS geometries of 1-propanol and 2-propanol reactions and calculated the energy of hydroxypropyl moiety at this geometry at the CBS-QB3 level of theory. The minimum energy structures of the hydroxypropyl radical products for each reaction were also optimized and their energy was calculated at the same level of theory. The energy difference between the vertical and adiabatic radical products from the H-abstraction is 2.0 kcal mol^{-1} for 2-propanol, and 2.7 kcal mol^{-1} or 3.1 kcal mol^{-1} for 1-propanol with α-H or β-H abstraction. The major geometry changes accounting for this difference are summarized in Table 2. For instance, the H-C-C-C dihedral angle changes from ~56° to ~42° in 1-propanol by α-H abstraction and changes from ~134° to ~165° in by β-H abstraction. The O-C-C-C dihedral angle changes from ~130° to ~143° in 2-propanol during the H abstraction. These significant geometric changes as listed in Table 2 give rise to certain vibrational excitation in the hydroxypropyl radicals, which could account for about 10%-30% of the total available energy depending on the collision energy.

We are expecting most of the total available energy (~30%-50%) is partitioned into the rotational excitation of the radical products, especially OH $X^2\Pi$ radical, whose rotational constant is large (18.91 cm^{-1})[42]. The rotational excitation of the OH radicals is induced by the long-range dipole-dipole interaction between the OH and hydroxypropyl radicals. We calculated that OH has dipole moment of 1.815 D at the CBS-QB3 level of theory compared to the experimental measurement of 1.6676(9) D.[45] The dipole moments for CH_3CH_2CHOH, CH_3CHCH_2OH and $(CH_3)_2COH$ are calculated to be 1.282, 2.182, and 1.653 D at the same level of theory. The long-range dipole-dipole interaction between the strong polar product pair is also supported by the presence of the post-TS exit channel complex (bound by 3-5 kcal mol^{-1}) in all H abstraction pathways on the potentials as shown in Figure 4. This dipole-dipole interaction will induce the reorientation of the radical pair, after passage through the reaction TS and prior to separation to form products, resulting in the rotational excitation of both products. Orr-Ewing and coworkers systemically studied this post-TS dipole-dipole interaction effect by comparing the rotational product state distributions of HCl from the Cl atom reaction with alkane and oxygen-containing organic compounds.[15, 18] The rotationally cold HCl product (peaking at J=0,1) was probed (governed by the collinear Cl-H-C structure in TS) for the reaction of Cl with alkane, where the interaction is weak between the polar HCl and the non-polar alkyl radical.[15] However, more rotational excitation of HCl is observed (peaking at J=3-5) for the Cl + methanol, ethanol, dimethyl ether reactions (despite of the collinear Cl-H-C geometry in TS), where the interaction is strong between both polar products.[18] Very recently, our group studied the bimolecular reaction dynamics of $O(^3P)$ reaction with aliphatic amines (dimethylamine and trimethylamine), and found that the dipole-dipole interaction of the strong polar OH and aminoalkyl product radicals plays an important role in promoting the occurrence of intersystem crossing in the exit channel.[19]

CONCLUSION

We have performed an imaging study of the reaction dynamics of ground state atomic oxygen with propanol isomers under single collision conditions with well-defined collision energies of 8 and 10 kcal mol^{-1}. The hydroxypropyl radical products, generated from the α-H and β-H abstraction for 1-propanol and α-H abstraction for 2-propanol, were detected with our universal VUV (157 nm) soft ionization probe with velocity map imaging technique. The global differential cross sections and translational energy distributions were obtained from these images. Backward-sideways scattering but more pronounced backward scattering was observed for both propanol isomer reactions under two different collision energy in the experiment. Low average translational energy release was obtained, accounting for 20%-40% of the total available energy, which indicates that a large amount of energy is released as the internal excitation of the products. Previous OH product state measurements in the relevant reactions suggest that the vibrational excitation of OH radical could take about 10%-30% of the total available energy. A modification of the triatomic model, called as "vertical" H abstraction mechanism, was applied to estimate the internal excitation of the hydroxypropyl radical that accounts for about 10%-30% of the total available energy. Most of the total available energy (~30%-50%) is partitioned into the rotational excitation of the OH radicals due to the strong long-range dipole-dipole interaction between the dipolar OH and hydroxypropyl radicals. This post-transition state dipole-dipole interaction may play an important role in the H-abstraction or other types of reaction dynamics in more polyatomic systems.

ACKNOWLEDGMENTS

This work was supported by the Director, Office of Science, Office of Basic Energy Science, Division of Chemical Science, Geoscience and Bioscience of the U.S. Department of Energy under Contract No.DE-SC0017130.

Table 1. Summary of results on the translational energy partitioning for O(^{3}P) + propanol isomers

	E_c[a]	E_{avl}[b]	$\langle E_T \rangle$ SW[c]	$\langle E_T \rangle$ BW[d]	$\langle E_T \rangle/E_c$ SW[e]	$\langle E_T \rangle/E_c$ BW[f]	$\langle E_T \rangle/E_{avl}$ SW[g]	$\langle E_T \rangle/E_{avl}$ BW[h]
1-Propanol	8.1	15.9[i]	3.25	3.81	0.41	0.48	0.20[i]	0.24[i]
		11.5[j]					0.28[j]	0.33[j]
	10.2	18.0[i]	4.75	5.3	0.46	0.51	0.26[i]	0.29[i]
		13.6[j]					0.35[j]	0.39[j]
2-Propanol	8.3	18.2	3.51	4.26	0.42	0.51	0.19	0.23
	10.0	19.9	4.76	5.45	0.48	0.55	0.24	0.27

[a]Collision energy. [b]Total available energy (collision energy + reaction energy release calculated by CBS-QB3 level of theory). [c]Average translational energy in the sideways direction. [d]Average translational energy in the backward direction. [e]Fraction of collision energy appearing in translation of the sideways component. [f]Fraction of collision energy appearing in translation of the backward component. [g]Fraction of total available energy appearing in translation of the sideways component. [h]Fraction of total available energy appearing in translation of the backward component. [i]Results from α-H abstraction site of 1-propanol. [j]Results from β-H abstraction site of 1-propanol.

Table 2. Results of ab initio calculations performed as described in the text (hartrees, degrees, angstroms).

	$CH_3CH_2CHOH^*$	$CH_3CH_2CHOH^\bullet$	$CH_3CHCH_2OH^*$	$CH_3CHCH_2OH^\bullet$	$(CH_3)_2COH^*$	$(CH_3)_2COH^\bullet$
Energy	-193.341527	-193.345812	-193.333696	-193.338695	-193.351559	-193.354680
∠OC1C2	110.7°	114.5°	-	-	-	-
∠C1C2C3	-	-	116.5°	121.4°	115.9°	121.4°
∠OC1C2C3	176.6°	170.8°	178.7°	166.6°	129.7°	143.1°
∠HC1C2C3	55.6°	41.9°	134.1°	165.3	-	-
O-C1/O-C2[◊]	1.394	1.375	-	-	1.396	1.383
C1-C2	1.514	1.488	1.506	1.484	1.515	1.495
C2-C3	-	-	1.511	1.489	1.515	1.490

[*]The radical structure at the geometry of its parent molecule. [•]The lowest energy structure of the radical. [◊]Bond length of O-C1 for CH_3CH_2CHOH and bond length of O-C2 for $(CH_3)_2COH$.

REFERENCES:

1. W. C. J. Gardiner, *Combustion Chemistry*, Springer-Verlag New York, 1984.
2. B. J. Finlayson-Pitts and J. N. Pitts, *Chemistry of the Upper and Lower Atmosphere*, Academic Press, San Diego, 2000.
3. A. Dalgarno and J. H. Black, *Rep. Prog. Phys.*, 1976, **39**, 573.
4. P. Casavecchia, F. Leonori and N. Balucani, *Int. Rev. Phys. Chem.*, 2015, **34**, 161-204.
5. Y. T. Lee, *Science*, 1987, **236**, 793.
6. X. M. Yang and D. H. Zhang, *Acc. Chem. Res.*, 2008, **41**, 981-989.
7. H. Pan, K. Liu, A. Caracciolo and P. Casavecchia, *Chem. Soc. Rev.*, 2017, **46**, 7517-7547.
8. F. Ausfelder and K. G. McKendrick, *Prog. React. Kinet. Mec.*, 2000, **25**, 299-370.
9. P. Andresen and A. C. Luntz, *J. Chem. Phys.*, 1980, **72**, 5842-5850.
10. A. C. Luntz and P. Andresen, *J. Chem. Phys.*, 1980, **72**, 5851-5856.
11. N. J. Dutton, I. W. Fletcher and J. C. Whitehead, *Mol. Phys.*, 1984, **52**, 475-483.
12. G. M. Sweeney, A. Watson and K. G. McKendrick, *J. Chem. Phys.*, 1997, **106**, 9172-9181.
13. H. Tsurumaki, Y. Fujimura and O. Kajimoto, *J. Chem. Phys.*, 2000, **112**, 8338-8346.
14. X. H. Liu, R. L. Gross, G. E. Hall, J. T. Muckerman and A. G. Suits, *J. Chem. Phys.*, 2002, **117**, 7947-7959.
15. C. Murray and A. J. Orr-Ewing, *Int. Rev. Phys. Chem.*, 2004, **23**, 435-482.
16. S. Rudić, C. Murray, J. N. Harvey and A. J. Orr-Ewing, *Phys. Chem. Chem. Phys.*, 2003, **5**, 1205-1212.
17. C. Murray, A. J. Orr-Ewing, R. L. Toomes and T. N. Kitsopoulos, *J. Chem. Phys.*, 2004, **120**, 2230-2237.
18. S. Rudić, C. Murray, D. Ascenzi, H. Anderson, J. N. Harvey and A. J. Orr-Ewing, *J. Chem. Phys.*, 2002, **117**, 5692-5706.
19. H. Li, A. Kamasah, S. Matsika and A. G. Suits, *Nat. Chem.*, 2018, in press.
20. M. Ahmed, D. Blunt, D. Chen and A. G. Suits, *J. Chem. Phys.*, 1997, **106**, 7617-7624.
21. D. W. Chandler and P. L. Houston, *J. Chem. Phys.*, 1987, **87**, 1445-1447.
22. A. T. J. B. Eppink and D. H. Parker, *Rev. Sci. Instrum.*, 1997, **68**, 3477-3484.
23. D. Townsend, M. P. Minitti and A. G. Suits, *Rev. Sci. Instrum.*, 2003, **74**, 2530-2539.

24. B. Joalland, Y. Y. Shi, A. D. Estillore, A. Kamasah, A. M. Mebel and A. G. Suits, *J. Phys. Chem. A*, 2014, **118**, 9281-9295.
25. M. Kawasaki and H. Sato, *Chem. Phys. Lett.*, 1987, **139**, 585-588.
26. P. Felder, C. S. Effenhauser, B. M. Haas and J. R. Huber, *Chem. Phys. Lett.*, 1988, **148**, 417-422.
27. W. Li, S. D. Chambreau, S. A. Lahankar and A. G. Suits, *Rev. Sci. Instrum.*, 2005, **76**.
28. J. O. F. Thompson, C. Amarasinghe, C. D. Foley and A. G. Suits, *J. Chem. Phys.*, 2017, **147**, 013913.
29. J. O. F. Thompson, C. Amarasinghe, C. D. Foley, N. Rombes, Z. Gao, S. N. Vogels, S. Y. T. van de Meerakker and A. G. Suits, *J. Chem. Phys.*, 2017, **147**, 074201.
30. M. J. Frisch, G. W. Trucks, H. B. Schlegel, G. E. Scuseria, M. A. Robb, J. R. Cheeseman, G. Scalmani, V. Barone, G. A. Petersson, H. Nakatsuji, X. Li, M. Caricato, A. V. Marenich, J. Bloino, B. G. Janesko, R. Gomperts, B. Mennucci, H. P. Hratchian, J. V. Ortiz, A. F. Izmaylov, J. L. Sonnenberg, D. Williams-Young, F. Ding, F. Lipparini, F. Egidi, J. Goings, B. Peng, A. Petrone, T. Henderson, D. Ranasinghe, V. G. Zakrzewski, J. Gao, N. Rega, G. Zheng, W. Liang, M. Hada, M. Ehara, K. Toyota, R. Fukuda, J. Hasegawa, M. Ishida, T. Nakajima, Y. Honda, O. Kitao, H. Nakai, T. Vreven, K. Throssell, J. A. J. A. Montgomery, J. Peralta, J. E. , F. Ogliaro, M. J. Bearpark, J. J. Heyd, E. N. Brothers, K. N. Kudin, V. N. Staroverov, T. A. Keith, R. Kobayashi, J. Normand, K. Raghavachari, A. P. Rendell, J. C. Burant, S. S. Iyengar, J. Tomasi, M. Cossi, J. M. Millam, M. Klene, C. Adamo, R. Cammi, J. W. Ochterski, R. L. Martin, K. Morokuma, O. Farkas, J. B. Foresman and D. J. Fox, *Gaussian 16, Revision A.03 (Gaussian, Inc., Wallingford CT, 2016)*.
31. B. Joalland, Y. Shi, A. Kamasah, A. G. Suits and A. M. Mebel, *Nat. Commun.*, 2014, **5**.
32. D. L. Proctor and H. F. Davis, *Proc. Natl. Acad. Sci. U.S.A.*, 2008, **105**, 12673-12677.
33. R. Z. Hinrichs, J. J. Schroden and H. F. Davis, *J. Am. Chem. Soc.*, 2003, **125**, 860-861.
34. X. Gu and R. I. Kaiser, *Acc. Chem. Res.*, 2009, **42**, 290-302.
35. N. Balucani, F. Zhang and R. I. Kaiser, *Chem. Rev.*, 2010, **110**, 5107-5127.
36. R. I. Kaiser and A. M. Mebel, *Chem. Soc. Rev.*, 2012, **41**, 5490-5501.
37. Y. Shi, A. Kamasah and A. G. Suits, *J. Phys. Chem. A*, 2016, **120**, 8933-8940.
38. T. J. Lee and P. R. Taylor, *Int. J. Quantum Chem.*, 1989, **36**, 199-207.

39. A. L. Ayub and J. M. Roscoe, *Can. J. Chem.*, 1979, **57**, 1269-1273.
40. G. E. Busch and K. R. Wilson, *J. Chem. Phys.*, 1972, **56**, 3626-3638.
41. G. T. Evans, E. van Kleef and S. Stolte, *J. Chem. Phys.*, 1990, **93**, 4874-4883.
42. J. P. Maillard, J. Chauville and A. W. Mantz, *J. Mol. Spectrosc.*, 1976, **63**, 120-141.
43. N. J. Dutton, I. W. Fletcher and J. C. Whitehead, *J. Phys. Chem.*, 1985, **89**, 569-570.
44. E. S. Whitney, A. M. Zolot, A. B. McCoy, J. S. Francisco and D. J. Nesbitt, *J. Chem. Phys.*, 2005, **122**, 124310.
45. W. L. Meerts and A. Dymanus, *Chem. Phys. Lett.*, 1973, **23**, 45-47.

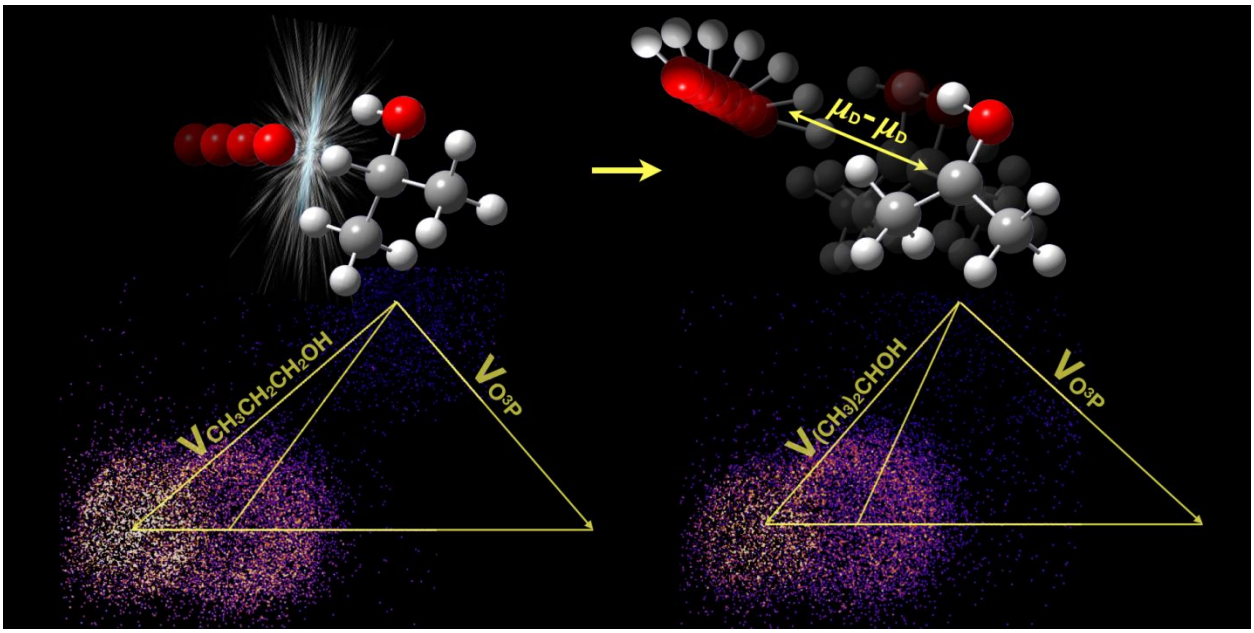

TOC: Direct rebound dynamics are revealed for bimolecular reaction of the ground state O(^{3}P) atom with propanol isomers, involving the post transition state long-range dipole-dipole interaction between the dipolar OH and hydroxypropyl radicals.